Thermally Induced Gelation of Poly(acrylamide) Grafted with Poly(*N*-isopropylacrylamide): A Small-Angle Neutron Scattering Study

Valessa Barbier,[†,‡] Mélanie Hervé,[§] Jan Sudor,[‡] Annie Brulet,[||] Dominique Hourdet,[§] and Jean-Louis Viovy*[,†]

Laboratoire de physico-chimie Curie (UMR 168), Institut Curie, section de recherche, 11, rue Pierre et Marie Curie, 75231 Paris Cedex 05, France, Laboratoire de Physico-Chimie des Polymères et des Milieux Dispersés, UMR 7615 (ESPCI − CNRS − UPMC), 10, rue Vauquelin, 75231 Paris Cedex 05, France, Laboratoire Léon Brillouin, CEA-Saclay, 91191 Gif-sur-Yvette Cedex, France, and Laboratoire MicroSystèmes pour la Biologie, CEA-LETI/DSIS/SSBS, 17 rue des Martyrs, 38054 Grenoble Cedex 9, France

Received April 27, 2004

ABSTRACT: Sieving matrixes of poly(acrylamide) grafted with poly(*N*-isopropylacrylamide) (PNIPAM) were developed in the framework of DNA sequencing by capillary electrophoresis. As a result of their thermodynamic properties, PNIPAM side chains self-aggregate above a critical temperature, leading to strong thermo-thickening effects in semidilute solutions. We report here a study of the transient network formation, carried out in D_2O by small-angle neutron scattering on the basis of a large set of responsive copolymers tailored with PNIPAM grafts of different sizes (M_w = 10 000, 20 000, and 35 000 g/mol) and various graft densities (5, 7, 10, 14, and 18% w/w). For most of the aqueous solutions, a correlation peak is observed at finite scattering vectors when the temperature is increased above a critical value. The intensity of the scattering peak rises with the size of the PNIPAM stickers, the graft density, the concentration, and the temperature. Experimental data are fitted using a core−corona model, assuming that only part of PNIPAM grafts (f_{PNIPAM}, mass fraction) participate in the aggregation process (dry micelles). Under these assumptions, the five-parameter model allows a realistic description of the thermally induced association with core sizes ranging between 70 and 100 Å and f_{PNIPAM} varying between 18 and 50%, depending on the primary structure of the copolymers. Comparison between matrixes confirms that physical networks based on responsive aggregation are good candidates for DNA sequencing even if they display antagonistic properties arising from (1) an increase of the resolution due to the matrix gelation (especially for large DNA fragments) and (2) a dispersion of DNA fragments during separation due to specific interactions between hydrophobic domains and DNA, which results in a loss of resolution.

1. Introduction

Microphase separation in aqueous macromolecular solutions can lead to rich and complex rheological properties, and it proved to be very interesting for numerous applications in polymer science, in particular oil recovery, paint industry, drug delivery systems, and more recently biotechnologies (analysis, diagnostic, cell biology, etc.). Thermo-thickening polymers in particular (leading to an increase of viscosity with temperature) have attracted attention in the past decade as a result of their original behavior, which is opposite to the behavior of conventional liquids. Many applications can be envisioned, in which thermoassociating copolymers could be used to adjust the viscosity of the aqueous fluids. Although various thermoassociating systems have been reported in the literature,[1−4] a number of them such as methylcellulose or poly(*N*-isopropylacrylamide) (PNIPAM) give turbid solutions upon gelation. This signifies the presence of large heterogeneities on a micrometer scale, which could be detrimental to some applications. One possible strategy to obtain more homogeneous transient networks consists of preparing macromolecular architectures combining a water-soluble polymer backbone and responsive blocks or side chains having a LCST (lower critical solution temperature) in water.[5−8] Among LCST polymers, PNIPAM was extensively studied mainly because its transition temperature around 32 °C allows a responsive behavior in the vicinity of room and body temperatures. Previously reported macromolecular systems involving PNIPAM as responsive stickers include poly(acrylic acid) grafted with PNIPAM[9] and PNIPAM grafted with poly(ethylene oxide) (PEO).[10−11] Those grafted copolymers form micelles with "core−shell" structures in aqueous solutions above their transition temperatures. [12]

As described in a previous article, we developed a new family of thermo-thickening polymers based on poly(acrylamide) (PAM) grafted with PNIPAM.[13] These copolymers consist of a water-soluble PAM backbone grafted with relatively small PNIPAM side chains. The synthesis of such copolymers (i.e., copolymerization of acrylamide (AM) with PNIPAM macromonomers bearing a single acrylic function at one end) leads to copolymer chains with a reasonable polydispersity (around 2) and allows for an independent control of the average molecular weights of the grafts and backbone and the grafting density.

When PNIPAM chains are incorporated into a macromolecular structure, they form micellelike aggregates at a temperature higher than the transition temperature T^* (>LCST) to minimize their contact with solvent. This results in a strong increase of the viscosity from ∼100 mPa·s to ∼10 000 mPa·s (Figure 1). Influence of the graft size and graft density on rheological behavior

* To whom correspondence should be addressed. E-mail: jean-louis.viovy@curie.fr.
† Institut Curie, section de recherche.
‡ UMR 7615 (ESPCI − CNRS − UPMC).
§ CEA-Saclay.
|| CEA-LETI/DSIS/SSBS.

10.1021/ma049182y CCC: $27.50
Published on Web 07/02/2004

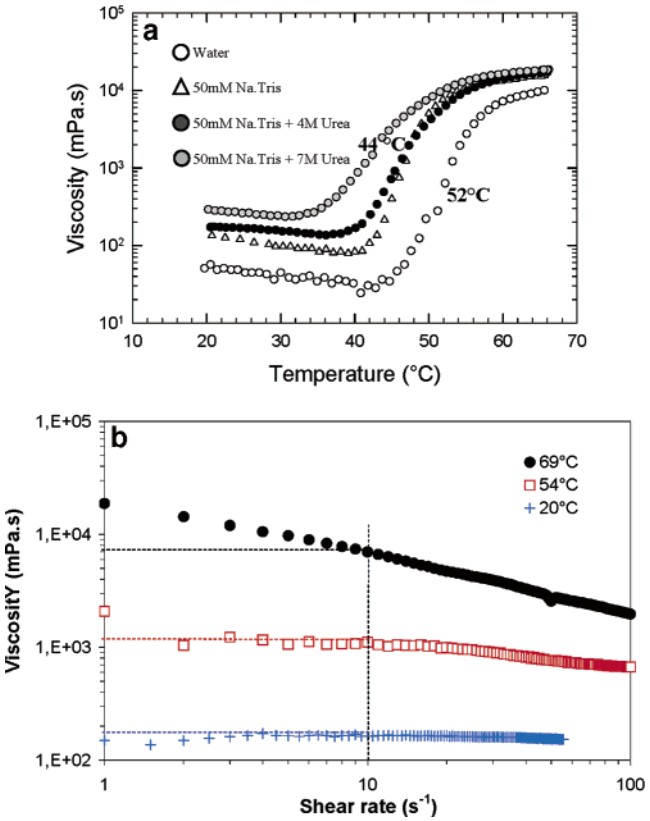

Figure 1. Viscosity measurements, with a Brookfield DV-III rheometer. (a) Viscosity versus temperature; heating rate 2 °C/min; P(AM1500−NIPAM10/10%), 3% in milli-Q deionized water, 50 mM Na Tris, 50 mM Na Tris + 4 M urea, 50 mM Na Tris + 7 M urea; shear rate = 10 s^{-1}; from eq 11. (b) Viscosity versus shear rate at 24, 54, and 69 °C; P(AM1500−NIPAM10/10%), 3% in milli-Q deionized water.

and transition temperature has been studied previously.[13] Keeping a constant graft density, that is, identical AM/PNIPAM mass ratio, *T** increases strongly with the graft size up to molecular weights of 15 000 Da and then becomes graft-size independent. Indeed, it has been shown that shorter chains present a smaller enthalpic contribution to the free energy of solubilization, and, therefore, their solvation is favored compared to that of bigger chains.[7] It has also been observed that *T** decreases with increasing graft density, that is, the amount of PNIPAM in a copolymer.[13] The same trend has been observed with PNIPAM−PEO.[11] The amplitude of the thermo-thickening is rather independent of the product of the graft size and graft density. This suggests that the overall interaction strength increases with an increasing graft size and an increasing grafting density.

P(AM-*g*-PNIPAM) copolymers are electroneutral and, thus, less sensitive to pH or salt concentration than charged thermo-thickeners. Aqueous solutions of these copolymers are clear upon gelation. Although they were specially developed for the use as sieving media for DNA sequencing by capillary electrophoresis, they can probably be interesting for other applications as well. For instance, the thermo-thickening properties of P(AM-*g*-PNIPAM) could be very useful for lab-on-a-chip applications because aqueous solutions of such copolymers can be easily injected into small diameter channels thanks to the thermal switching between low- and high-viscosity states through a modest increase in temperature (∼20 °C).

Table 1. Molar Mass M_w (g/mol) and Polydispersity I_p of PNIPAM Macromonomers

name	PNIPAM10	PNIPAM15	PNIPAM20	PNIPAM35
M_w (g/mol)	10 800	15 800	23 000	34 000
I_p (M_w/M_n)	5.7	4.2	4.9	5

Many hydrophilic matrixes, such as PAM, cellulose derivatives (methylethylcellulose, hydroxyethylcellulose, etc.),[14,15] poly(*N*,*N*-dimethylacrylamide) (PDMA),[16] PEO,[17] and poly(vinylpyrrolidone),[18] have been used for DNA separations by capillary electrophoresis. The matrixes for DNA separations have been currently reviewed in refs 19−21 while thermoresponsive and shear-responsive polymer solutions with "switchable" viscosities were described in ref 22. It has been shown that linear polyacrylamide (LPA) based separation matrixes give the longest read lengths in DNA sequencing.[23−26] Unfortunately, the high-molecular-weight LPA solutions required for long read lengths are very viscous, and their injection into small-diameter channels remains quite challenging. To overcome this challenge, several research groups have developed either low or switchable viscosity matrixes. The thermo-associative matrixes used in capillary electrophoresis separations are, for instance, PNIPAM grafted with PEO,[27] mixtures of poly(butylene oxide) (PBO)−PEO−PBO,[28] and triblock copolymers made of PEO and poly(propylene oxide) (PPO; Pluronic F127).[29−30] Pluronics form spherical micelles with a hydrophobic core of PPO blocks and a hydrated PEO shell. The structure of pluronics systems has been studied by small-angle neutron scattering (SANS) and numerical simulations employing a core−corona model.[31−35]

In this work, we report SANS experiments performed with aqueous P(AM-*g*-PNIPAM) solutions. Thanks to the strong contrast in the scattering length density (SLD) between hydrogen and deuterium, SANS is a powerful method to probe the microstructure of hydrogenated polymers in D_2O solutions, and it has been used with success in the past to study associative polymers.[32,35−37] To explore the influence of the primary structure on the associating process, we studied the transient network formation of copolymers tailored with different graft sizes and different graft densities at various temperatures (i.e., under and above the critical temperature *T**).

2. Material and Methods

Polymer Synthesis. The P(AM-*g*-PNIPAM) copolymers were synthesized by radical aqueous polymerization and characterized in our laboratory. The protocol is described in ref 13. The molar masses and fractions of PNIPAM incorporated are given Tables 1 and 2.

Viscosity Measurements. Viscosity measurements were performed with a Brookfield DV-III rheometer.

The influence of temperature was studied with a P(AM1500−NIPAM10/10%) 3% (w/v) solution in water, 50 mM Na Tris buffer, in 50 mM Na Tris buffer + 4 M urea, and in 50 mM Na Tris buffer + 7 M urea. The shear rate was 10 s^{-1}. Then, influence of the shear rate was studied at three different temperatures, under (20 °C), around (54 °C), and above (69 °C) the transition temperature (see section 4, Rheological Behavior). We used a P(AM1500−NIPAM10/10%) 3% (w/v) solution in water, and the shear rate was varied from 1 to 100 s^{-1}.

Differential Scanning Calorimetry (DSC). The dehydration of PNIPAM chains as the temperature increases has been studied by DSC. In such experiments, the dehydration process between PNIPAM and water gives rise to an endot-

Table 2. Primary Structure of Grafted Copolymers: Incorporated Macromonomer, Graft Density (Mass %), Molar Mass M_w (g/mol), and Polydispersity I_p

copolymer	macromonomer	graft density (mass %)	M_w (g/mol)	I_p
P(AM2000−NIPAM15/10%)	PNIPAM15	10.11	1.8×10^{6a}	3.9
P(AM1500−NIPAM15/10%)	PNIPAM15	10.14	1.4×10^{6a}	6.6
P(AM700−NIPAM15/10%)	PNIPAM15	10.38	6.5×10^{5a}	5.5
P(AM1500−NIPAM10/10%)	PNIPAM10	10.16	1.5×10^{6}	1.5
P(AM1500−NIPAM20/10%)	PNIPAM20	10.19	1.5×10^{6a}	4.7
P(AM1500−NIPAM35/10%)	PNIPAM35	9.15	1.0×10^{6a}	5.1
P(AM1500−NIPAM10/5%)	PNIPAM10	5.26	1.5×10^{6}	1.6
P(AM1500−NIPAM10/7%)	PNIPAM10	7.49	1.1×10^{6}	1.6
P(AM1500−NIPAM10/14%)	PNIPAM10	13.93	2.3×10^{6}	1.7
P(AM1500−NIPAM10/18%)	PNIPAM10	17.70	2.1×10^{6}	1.8
P(AM1500−NIPAM15/14%)	PNIPAM15	14.46	1.3×10^{6}	2
P(AM1500−NIPAM15/18%)	PNIPAM15	18.11	$\sim 1.3 \times 10^{6}$	

[a] In PEO equivalents (calibration made with PEO standards).

hermic peak in the LCST range. We compared the dehydration enthalpy between PNIPAM grafted on a PAM backbone and free PNIPAM chains. Two samples were analyzed: (i) PNIPAM10 at 0.3% in milli-Q water and (ii) P(AM1500−NIPAM10/10%) at 3% (w/v) in milli-Q water. We considered, in the first case, free PNIPAM chains in solution and, in the second case, PNIPAM grafted on the PAM backbone. In both cases, the same amount of PNIPAM is analyzed.

DNA Separation. In section 4, we report separation performances of P(AM1500−NIPAM10/10%). The influence of temperature on peak dispersion and comparison of the matrix with commercial matrixes are presented. These experiments have been made with a single-stranded DNA (ssDNA) "ladder" with fragments 100, 200, 300, 400, 500, 600, 700, 800, 1000, 1250, and 1500 bases long singly labeled with fluorescein (BioVentures, Murfreesboro, TN). DNA samples were mixed with formamide (50:50 v/v), heated 5 min at 95 °C, and rapidly cooled on ice prior to their injection. The separations of the DNA samples were performed on an ABI 310 instrument at 50 °C (except for the study involving the temperature's influence). P(AM1500−NIPAM10/10%) 3% (w/v) solutions were prepared in 50 mM Tris-aminopropanesulfonic acid, 50 mM Tris, 2 mM ethylenediaminetetraacetic acid, and 7 M urea (denaturating agent).

The separation performance is evaluated in terms of resolution R_s[38] [eq 1; peak spacing per base (PS) divided by the peak width at half-height (PW)]. PS reflects the separation power of the matrix and PW is related to the peak dispersion. Both are expressed in length units (mm).

$$R_s = \frac{1}{4}\left|\frac{\Delta\mu}{\mu_{av}}\right| N^{1/2} \tag{1a}$$

with

$$\left|\frac{\Delta\mu}{\mu_{av}}\right| = 2\left|\frac{t_{m1} - t_{m2}}{t_{m1} + t_{m2}}\right| \tag{1b}$$

and

$$N = 5.5\left(\frac{t_m}{\varpi_{1/2}}\right)^2 = 5.5\left[\frac{(t_{m1} + t_{m2})/2}{\varpi_{1/2}}\right]^2 \tag{1c}$$

R_s can also be written as

$$R_s = 0.59\left[\frac{(t_{m2} - t_{m1})/(N_2 - N_1)}{\varpi_{1/2}}\right] = 0.59\left(\frac{PS}{PW}\right) \tag{1d}$$

SANS Experiments. SANS experiments were performed at the Laboratoire Leon Brillouin, Saclay, France. The neutron wavelength λ used was 12 Å, and the sample-to-detector distance was set to 4.5 m. The corresponding scattering vector

$$q = \frac{4\pi}{\lambda}\sin\left(\frac{\theta}{2}\right) \tag{2}$$

was varied in the range 0.0034−0.0365 Å^{-1}. θ is the scattering angle.

Table 3. Experimental Parameters: Mass Concentration of the Polymer Solution, Temperature, and Peak Maximum Position q_{max}

copolymer	mass concentration (%)	temperature (°C)	q_{max} (Å^{-1})
P(AM1500−NIPAM10/5%)	5	33	no peak
P(AM1500−NIPAM10/5%)	5	59	0.0057
P(AM1500−NIPAM10/5%)	5	71	0.0069
P(AM1500−NIPAM10/7%)	5	59	0.0066
P(AM1500−NIPAM10/10%)	5	59	0.0083
P(AM1500−NIPAM10/10%)	3	59	0.0066
P(AM1500−NIPAM20/10%)	5	59	0.0078
P(AM1500−NIPAM35/10%)	5	59	0.0066
P(AM1500−NIPAM10/14%)	5	59	0.01
P(AM1500−NIPAM10/18%)	5	59	0.0111

The copolymer's structural parameters, that is, the size of grafts (10 000, 20 000, and 35 000 g/mol), and the grafting density (5, 7, 10, and 18% w/w) were investigated in this study (Tables 1 and 2). Samples were dissolved in D_2O at room temperature and transferred into 5-mm-thick quartz containers for SANS experiments. The copolymer's concentration/structure relation (3 and 5% w/v) was investigated on P(AM1500−NIPAM10/10%) solutions, while the effect of temperature (33 °C < T^*, 59 °C ∼ T^*, and 71 °C > T^*) on the copolymer's structure was investigated on P(AM1500−NIPAM10/5%) (see Table 3). Note that the second copolymer has relatively short PNIPAM grafts and, consequently, its viscosity transition temperature (59 °C) is significantly higher than the LCST of pure, long-chain PNIPAM (32 °C).

To obtain the coherent scattering intensity of the copolymer, the signal given by a pure D2O sample, used as background, is subtracted from the scattering intensity of the copolymer sample. The efficiency of the detector cell was normalized by the intensity delivered by a pure water cell of 1-mm thickness.

Absolute measurements of the scattering intensity $I(q)$ (Å^{-1}) were obtained from the direct determination of the incident neutron beam flow and the cell solid angle.[39]

3. SANS Model

We consider a solution of a grafted copolymer, and at studied concentrations (>overlap concentration), the polymer chains are entangled. At a higher temperature than the transition temperature T^*, grafts become insoluble and tend to aggregate. As a result, we have an entangled polymer solution containing aggregates that are linked to each other.

Compared to block associating copolymers that have been studied several times,[32−35] the literature is poorer

Table 4. SLD of PAM, PNIPAM, and D_2O[a]

name	SLD (Å^{-2})	name	SLD (Å^{-2})
PAM	4.191×10^{-6}	D_2O	6.406×10^{-6}
PNIPAM	1.36×10^{-6}		

[a] For polymers, the nitrogen protons were assumed to be fast-exchanging so that the polymers are assumed to be bearing predominantly −ND and $-ND_2$ groups.

concerning graft copolymers.[37,40] Reference 37 deals with microphase separation in a semidilute solution of poly(sodium acrylate) grafted with PEO. The model used in the strong segregation regime indicated that PEO microdomains behave as polydisperse spherical micelles organized in a simple cubic lattice.

As in Hourdet et al.,[37] the shape of the peak and its small thickness suggest a short-distance potential interaction and strong interactions.

Several models have been used to give the most quantitative and accurate picture of the microstructure: (i) monodisperse PNIPAM-rich spherical micelles; (ii) polydisperse PNIPAM-rich spherical micelles; and (iii) core−corona (a PNIPAM-rich spherical core, surrounded by a corona enriched in PAM). In all cases, the results of the fits and mass conservation arguments led us to assume that only a fraction f_{PNIPAM} of grafts is involved in the aggregation process. This hypothesis is further explained in section 4.

In the case of spherical particles embedded in a continuous medium, the SANS scattering intensity is written as the product of a form factor, $F(q)$, and a structure factor, $S(q)$ (eq 3). $F(q)$ characterizes the form and shape of the aggregates whereas $S(q)$ describes the interactions between the aggregates:

$$I(q) = N_m(\Delta\rho)^2 F(q)\, S(q) \tag{3}$$

where N_m is the number of micelles per unit of volume and $\Delta\rho$ is the contrast of the SLD. The different SLDs (PAM, PNIPAM, and D_2O) used to calculate $\Delta\rho$ are reported in Table 4.

The Percus−Yevick (PY) theory of scattering from individual spheres generally works well for short-ranged potentials. For a hard sphere, the PY structure factor is (eq 4)[41]

$$S(q) = 1/\left[1 + \frac{24\Phi_{HS}G(2qR_{HS})}{2qR_{HS}}\right] \tag{4}$$

where ϕ_{HS} is the hard sphere volume fraction, R_{HS} is the hard sphere radius (interaction distance), and G is a trigonometric function (eq 5):

$$G(A) = \alpha(\sin A - A\cos A)/A^2 + \beta[2A\sin A - (2 - A^2)\cos A - 2]/A^3 + \gamma\{-A^4\cos A + 4[(3A^2 - 6)\cos A + (A^3 - 6A)\sin A + 6]\}/A^5 \tag{5}$$

where α, β, and γ are

$$\alpha = (1 + 2\Phi_{HS})^2/(1 - \Phi_{HS})^4$$

$$\beta = -6\Phi_{HS}(1 + \Phi_{HS}/2)^2/(1 - \Phi_{HS})^4$$

$$\gamma = (\Phi_{HS}/2)(1 + 2\Phi_{HS})^2/(1 - \Phi_{HS})^4$$

The form factor describes the shape of the scattering particles. Its expression depends on a given model.

(i) Monodisperse. For monodisperse PNIPAM aggregates of radius R_m, the form factor is given by

$$F(q) = \left[\frac{4}{3}\pi {R_m}^3 \frac{3J_1(qR_m)}{qR_m}\right]^2 \tag{6}$$

where J_1 is the first-order spherical Bessel function:

$$J_1(x) = \frac{\sin x - x\cos x}{x^2} \tag{7}$$

Using the previously described structure factor (eq 4) and supposing "dry" micelles (negligible quantity of water in the micelle), this model has three fitting parameters: R_{HS}, R_m, and f_{PNIPAM}, the mass fraction of grafts involved in the aggregation process.

(ii) Polydisperse. We considered the PNIPAM micelle solution as a polydisperse solution of homogeneous spheres with an average radius R_m and a Gaussian size distribution $\omega(r)$. In that case, the form factor is given by (eq 8)

$$F(q) = \int_{R_m-5s}^{R_m+5s} f(q, r)\, \omega(r)\, \mathrm{d}r \tag{8}$$

where $f(q, r)$ is the form factor of a sphere of radius r (eq 6) and $\omega(r)$ is the Gaussian size distribution given by eq 9 and the function of the polydispersity s:

$$\omega(r) = \frac{1}{\sqrt{2\pi}s}\exp\left[-\frac{(r - R_m)^2}{2s^2}\right] \tag{9}$$

In this model, the polydispersity (s) is an additional parameter as compared to the previous model. So, this model has four parameters.

(iii) Core−Corona. This model has often been used to describe the micellar organization of triblock copolymers, PEO−PPO−PEO (Pluronics).[33,34] These copolymer micelles can be viewed as consisting of a PPO core with a PEO corona. The corresponding form factor describes the scattering due to the hard sphere interface between the core and the corona and between the corona and the solvent. In our case, the presence of solvent was allowed in the corona but not in the core:

$$(\Delta\rho)^2 F(q) = \left[\frac{4}{3}\pi {R_1}^3(\rho_1 - \rho_2)3\frac{J_1(qR_1)}{qR_1} + \frac{4}{3}\pi {R_2}^3(\rho_2 - \rho_s)3\frac{J_1(qR_2)}{qR_2}\right]^2 \tag{10}$$

where R_1 and R_2 are respectively the core and the corona radii (see Figure 2) and ρ_1, ρ_2, and ρ_s are respectively the SLDs of the core, the corona, and the solvent (calculated from Table 4).

This model has five fitting parameters: R_1, R_2, R_{HS}, $\alpha_{AM,corona}$ (volume fraction of PAM in the corona), and f_{PNIPAM}.

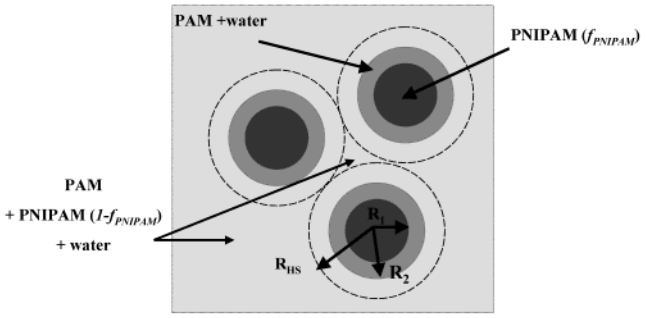

Figure 2. Model for core−corona micelles. We consider a dry PNIPAM core and an hydrated PAM corona. f_{PNIPAM} is the mass fraction of grafts involved in the aggregation process.

Knowing the core radius R_1, the number of grafts per aggregate N_{grafts} (eq 11) and, thus, the number of micelles per volume unit N_m (eq 12) can be determined:

$$N_{grafts} = \frac{^4/_3\pi {R_1}^3}{V_{PNIPAM}} \tag{11}$$

$$N_m = \frac{f_{PNIPAM} c \tau_w N_A}{M_{PNIPAM} N_{grafts}} \tag{12}$$

Where V_{PNIPAM} is the molar volume of PNIPAM (calculated from the molar volume of NIPAM), c is the copolymer concentration (mass %), τ_w is the graft density (mass %), $M_{PINIPAM}$ is the molar mass of PNIPAM, and N_A is the Avogadro number.

Knowing N_m, ϕ_{HS} is easily determined thanks eq 13:

$$\Phi_{HS} = \left(\frac{4}{3}\pi {R_{HS}}^3\right) N_m \tag{13}$$

4. Results and Discussion

Rheological Behavior. The rheological behavior of these grafted copolymers has been previously studied in our laboratory, and results are given in ref 13. Influence of graft density, graft size, and molecular weight and influence of the solvent (water, buffer, with or without urea) have been reported in this first article. The main conclusion is that this kind of copolymer presents a strong viscosifying effect, which should be due to the self-association of the hydrophobic parts (PNIPAM grafts) at high temperature. One can also notice that the solvent has a strong influence on the rheological behavior. Indeed, when adding buffer or urea (denaturing agent, necessary for ssDNA separation), the transition temperature is shifted to smaller values (Figure 1a).

To complete this study, we report here the variation of viscosity versus shear rate at different temperatures ($T < T^*$, $T \cong T^*$, and $T > T^*$). At low temperature, the copolymer solution behaves as a classical unassociated system (Figure 1b) and viscosity does not depend on shear rate. For a temperature higher than T^*, the viscosity seems to be shear-dependent as it is shown for 69 °C. It results probably from the competition between self-assembling of PNIPAM grafts under heating and stretching of the system under shearing.

Results from SANS Experimental Data. We investigated the structural properties of copolymers with different graft sizes and graft densities by SANS experiments. The presence of a correlation peak at a high temperature signaled the aggregation of LCST stickers, while the peak shape implied that the interactions between side chains were strong and repulsive. From Figure 3a,b we can see that the peak height increases with increasing graft density and graft size. This means that in both cases more PNIPAM is involved in aggregates. For a given size of the side-chains, the higher is the number of grafts in the copolymer chain, the higher is the probability for a PNIPAM chain to encounter in its vicinity a critical number of PNIPAM grafts to form a micelle and, thus, to get involved in an aggregate (entropic effect). This argument, however, seems to play against the increase of the peak intensity with graft length (because longer grafts are less numerous). We, thus, conclude that, in this case, the increase in aggregated fraction is controlled by the micellization enthalpy, which rules over the unfavorable entropic effect.

Concerning the copolymer with larger grafts (35 000 g/mol), no peak appears anymore in the q range explored but a strong scattering increase is observed at small values of q. This may be due to the heterogeneity of the sample: probably, these long grafts lead to a more complex structure, and the micelle model becomes irrelevant. Actually, these copolymers also lead to the poorest separation properties in electrophoresis, consistent with an increase in heterogeneities at large scales.

For P(AM1500−NIPAM 10/10%), two concentrations have been studied, 3% (w/v) and 5% (w/v; concentrations used for DNA separation by capillary electrophoresis; Figure 3c). At 5%, the peak is higher, which means more PNIPAM chains are involved in aggregates.

The effect of temperature has been studied with P(AM1500−NIPAM10/5%) (Figure 3d). At 35 °C, that is, under the association temperature T^*, there is no aggregate and no diffusion peak is observed. At 59 and 71 °C, a scattering peak the height of which increases with temperature demonstrates that aggregation is now effective. This shows that aggregates are either more numerous or larger (or both) at higher temperatures.

Hypothesis Resulting from DSC Experiments. The transition temperature T^* of the copolymer solution determined by using the maximum of the endothermic peak from DSC ($T \sim 47$ °C; see Figure 4b) compares quite well, considering the relative smoothness of the transition, with the value of 52 °C obtained from the rheological behavior (Figure 1). It can also be noticed that this temperature is somewhat higher that the one obtained in similar conditions with free PNIPAM macromonomers in solution (40 °C, Figure 4a). This shows that the difference between the temperature transition of the grafted macromonomer and the critical temperature of long PNIPAM chains (32 °C) is partly due to a finite-size effect and partly due to the attachment of the macromonomer onto a hydrophilic moiety. Such effects are well-known, for instance in the case of PEO−PPO block copolymers (pluronics).

Another important piece of information is that the total dehydration enthalpy of free PNIPAM macromonomers is about 15 times greater than the dehydration enthalpy of the same PNIPAM chains once incorporated in the copolymer (4 kJ/mol PNIPAM compared to 0.4 kJ/mol PNIPAM; Figure 4). Qualitatively, this result would be compatible with the two following assumptions: (i) PNIPAM cores are highly hydrated and (ii) only a fraction of the grafts are involved in the aggrega-

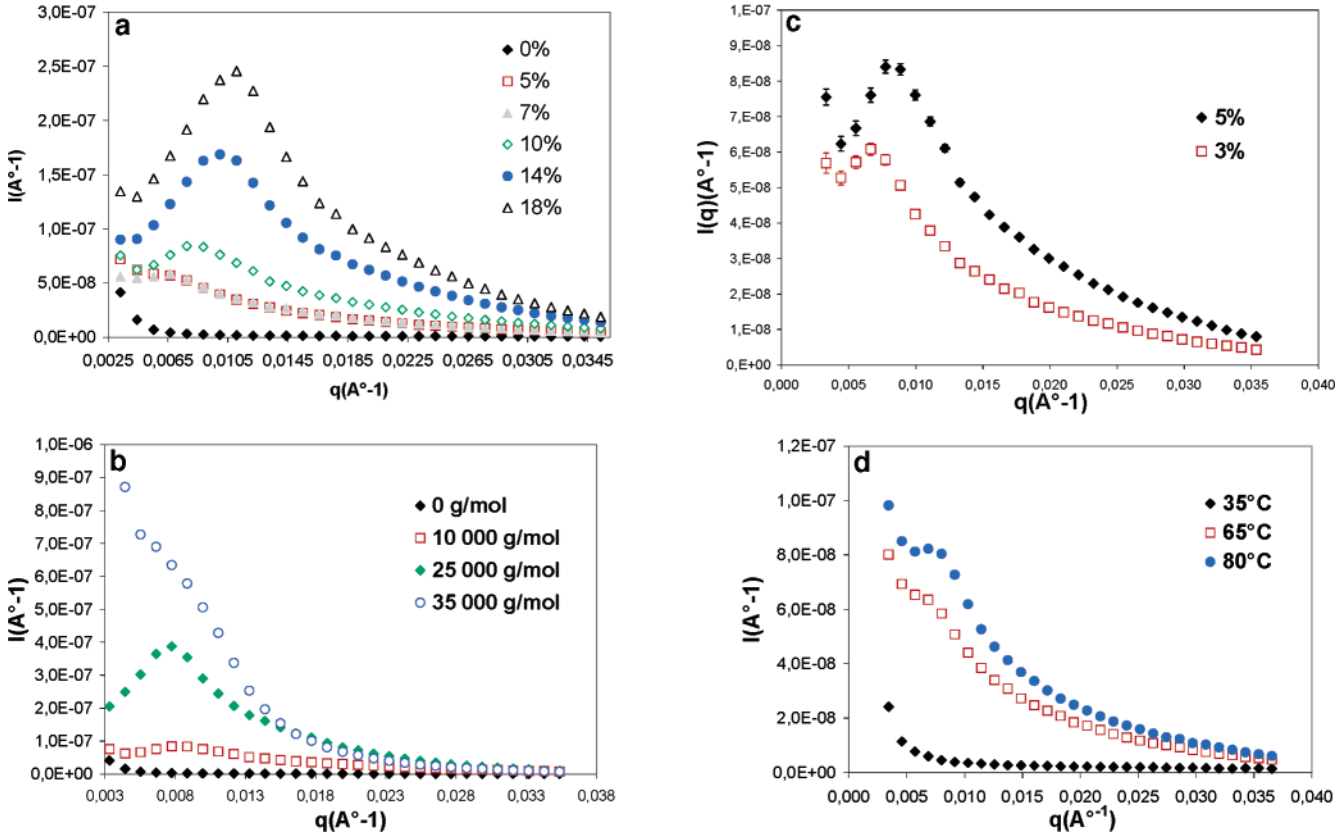

Figure 3. $I(q)$ (in $Å^{-1}$) versus q. Experimental data (normalized) in D_2O; influence of (a) graft density, 65 °C, 5%; (b) graft size, 65 °C, 5%; (c) concentration, 65 °C; and (d) temperature, 5%.

tion process. These two hypotheses will be reconsidered later, in light of the models used to fit quantitatively the neutron scattering data.

Comparison between Three Different Models Used To Fit SANS Data (Figure 5). Rather extensive literature exists on the SANS of block copolymer solutions, and in particular detailed core−corona models convincingly described the scattering of short diblock or triblock solutions.[33,34] The block copolymer system studied here is unfortunately more complex. As in the triblock polymer solutions, we can reasonably assume the presence of micellelike NIPAM aggregates with repulsive interactions. The intermicellar space, however, is more delicate to model. In the previously studied case of monodisperse "pluronic" triblock aggregates, the presence of well-defined hydrophilic "tails" made the hypothesis of a well-defined "corona" with uniform density of hydrophilic polymer reasonable. In our system, one can still assume that the chemical cross-link between the hydrophobic NIPAM blocks and the hydrophilic backbone plays the role of an attractive potential, leading to a high density of PAM surrounding the micelle. In contrast with pluronics systems, though, in our case the space between coronas is not void of PAM and the concentration of PAM in the water phase probably follows a rather complex and continuous distribution. No theoretical model is presently available for this distribution, so we decided to approximate it as a the combination of a spherical corona with a high density of PAM surrounding the micelle, floating in a continuous solution of polymer at a lower density. Actually, this approximation is probably not more dramatic than those previously used for pluronic systems because detailed models of polymer "brushes" show that the density profile is parabolic and not square, even for layers of monodisperse end-grafted polymers. This "core−corona" frame contains four independent geometrical parameters, the micelle diameter, the corona diameter, the hard core diameter, and the number density of micelles. Leaving all molar fractions of the two solutes PAM and NIPAM in the three compartments (hydrophobic core, corona, and continuous phase) totally free adds six more free parameters, but mass conservation reduces this number to four, knowing the polymer concentation and NIPAM/PAM molar fraction in pure polymer. Eight is an unrealistically high number of fitting parameters so that further assumptions are necessary to increase fit significance. It seems reasonable to further assume that the fraction of PAM in the hydrophobic core and the fraction of NIPAM in the corona are negligible. We are, thus, left with a six-parameters fit, involving a continuous phase with water, PAM, and NIPAM, micelle cores with hydrated NIPAM, and micelle coronas with hydrated PAM at a concentration different from this in the continuous phase.

This model can lead to satisfactory fits of most curves, but the fit is not robust to starting parameters, and equivalently good fits to the same curve could be obtained with quite diverse parameters sets. We conclude that six parameters are still too demanding on the fitting process, considering the quantity of data available, and the level of correlation between parameters in the phase space. We, thus, tried several further simplifications to reduce the number of parameters to five. As demonstrated in the following, assuming in addition that the core of the micelle is not hydrated does not significantly reduce fit quality but leads to a very stable and consistent fit, whereas all other five-parameter fits led to a poor fit or nonphysical fitting parameters.

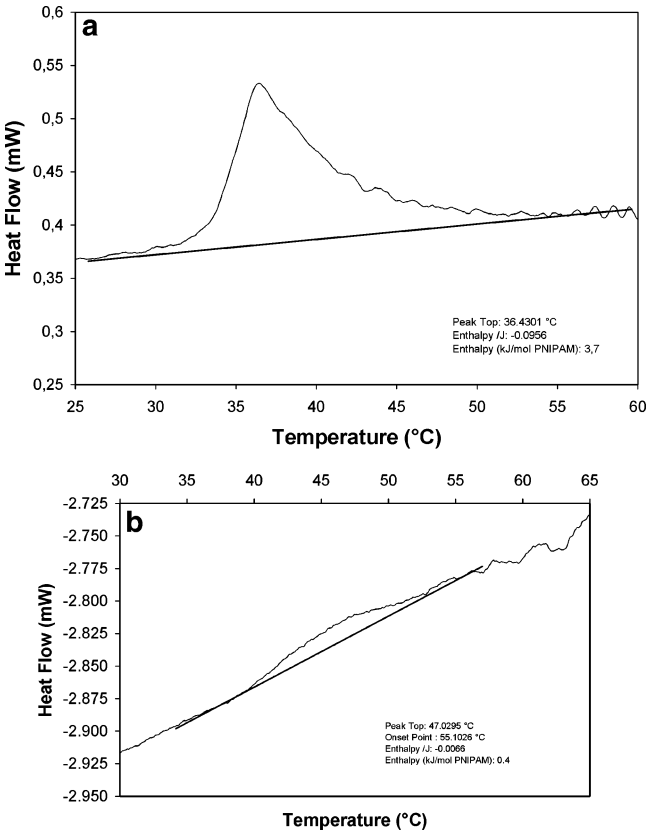

Figure 4. DSC measurements; measure of the exothermic activity: temperature is increased (1 °C/min); (a) PNIPAM10, 0.3% (w/v) in milli-Q water; (b) P(AM1500−NIPAM10/10%), 3% (w/v) in milli-Q water.

In the following part, we will use f_{PNIPAM} as the mass fraction of grafts involved in the aggregates, and we will consider these as dry PNIPAM micelles or "cores". Figure 5 shows the best-fit results with the different micellar models. The data shown correspond to P(AM1500−NIPAM10/18%), 5% (w/v) in D_2O, 59 °C. The core−corona model fits very well the experimental data, whereas the monodisperse model does not fit the data at all (it underestimates the peak height and its position is shifted to smaller q). The polydisperse model fits the experimental data rather well except for larger values of q. However, despite rather similar fit quality as compared to the core−corona model, the polydisperse model does not yield as consistent and physically reasonable best-fit parameters. In particular, the polydispersity is rather high and often larger than the average sphere radius. But, knowing PNIPAM side chains are themselves rather polydisperse, this possibility definitely cannot be excluded.

Anyway, in regard to the DSC results, we restrict the following discussion to the core−corona model, which seems the most satisfactory for our set of data.

SANS Data Analysis with the Core−Corona Model Considering a Dry Core and Only a Fraction of PNIPAM Grafts Participating in Micelles (Table 5). This model adjusts quite well the experimental data, especially for the copolymers with longer grafts and higher graft density, that is, for well-structured media (Figure 6). It allows us to determine for each copolymer the following fitting parameters: the core radius R_{core}, the corona radius R_{corona}, the hard-sphere radius R_{HS}, the volume fraction of PAM in the corona $\alpha_{AM,corona}$, and the mass fraction of PNIPAM involved in aggregation f_{PNIPAM} (Figure 7).

Effect of Graft Density. The number of grafts per aggregate decreases with increasing graft density (90 Å for a graft density of 5%, mass %, and 70 Å for 18%), and so does R_{core}). In contrast, micelles are more numerous as the graft density increases (1.5×10^{-10} micelles/Å^3 at 5% compared to 2.2×10^{-9} micelles/Å^3 at 18%), and so the hard-sphere radius decreases. Finally, the mass fraction of PNIPAM involved in aggregation increases with increasing graft density (f_{PNIPAM} = 18% for a graft density of 5% and 40% for a graft density of 18%, mass %).

Effect of Graft Size. First of all, the mass fraction of PNIPAM involved in aggregation increases with graft size (27% for 10 000 g/mol compared to 50% for 35 000

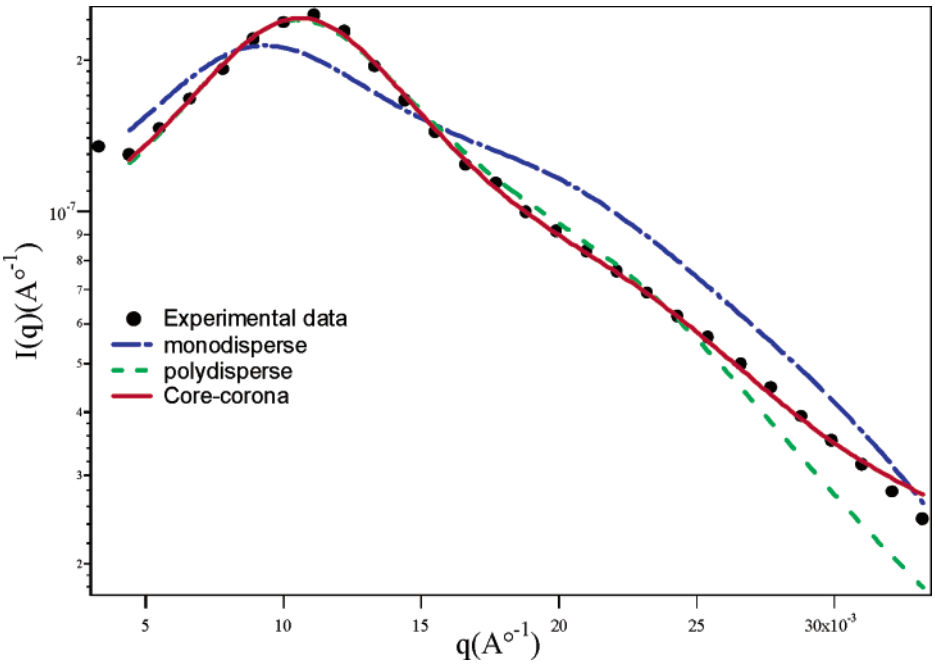

Figure 5. Fitting of the experimental $I(q)$ (in Å^{-1}) with monodisperse, polydisperse, and core−corona models, supposing the core is dry and only a fraction of grafts participate in the aggregation. Copolymer P(AM1500−NIPAM10/18%), 5% (w/v) in D_2O, 59 °C.

Table 5. Core−Corona Model Results[a]

copolymer	R_{core} (Å)	R_{corona} (Å)	R_{HS} (Å)	N_{grafts}	N_m	f_{PNIPAM} (%)	$\alpha_{AM,corona}$
P(AM1500−NIPAM10/5%)	90	290	398	177	1.52×10^{-10}	18	0.072
P(AM1500−NIPAM10/5%); 71 °C	86	273	345	157	2.70×10^{-10}	29	0.076
P(AM1500−NIPAM10/7%)	83	265	406	139	2.32×10^{-10}	16	0.074
P(AM1500−NIPAM10/10%), 3%	75	244	387	103	3.56×10^{-10}	23	0.066
P(AM1500−NIPAM10/10%)	70	213	310	86	8.35×10^{-10}	27	0.085
P(AM1500−NIPAM20/10%)	90	230	359	85	7.44×10^{-10}	47	0.130
P(AM1500−NIPAM35/10%)	98	248	276	73	5.57×10^{-10}	50	0.216
P(AM1500−NIPAM10/14%)	69	194	273	81	1.74×10^{-9}	36	0.104
P(AM1500−NIPAM10/18%)	71	191	252	89	2.22×10^{-9}	40	0.112

[a] R_{core}, core radius; R_{corona}, corona radius; R_{HS}, hard-sphere radius; N_{grafts}, number of grafts per micelle; N_m, number of micelles per unit of volume; f_{PNIPAM}, mass fraction of graft involved in aggregation; $\alpha_{AM,corona}$, volume fraction of AM in the corona. When not stated otherwise, the polymer solution is 5% and temperature is 59 °C.

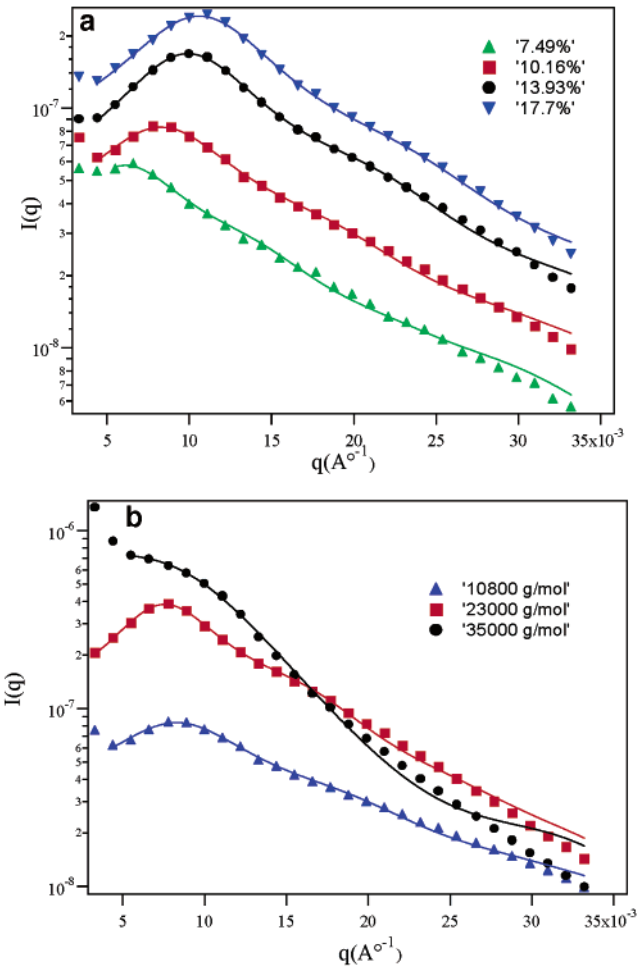

Figure 6. Fitting of the experimental $I(q)$ (in Å^{-1}) with the core−corona model: (a) varying graft density; (b) varying graft size.

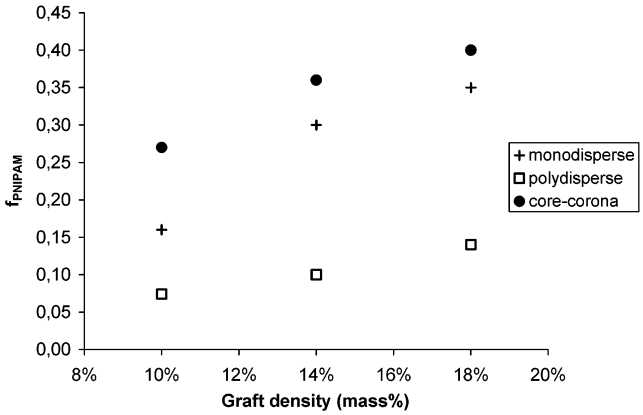

Figure 7. Mass fraction of PNIPAM involved in the aggregation process (f_{PNIPAM}) versus graft density. Results from the three different models: monodisperse, polydisperse, and core−corona.

g/mol). Indeed, polymer chains get less soluble as their size increases. Because the graft density, that is, mass fraction of PNIPAM, remains constant here, there are less grafts per chain when the graft size increases. As a result, the density of micelles decreases and the hard-sphere radius increases.

Effect of Concentration. The 3% and 5% solutions have been analyzed by SANS. With varying concentration, f_{PNIPAM} remains rather constant, but the number density of micelles increases from 3.5×10^{-10} at 3% to 8.4×10^{-10} at 5% [example given with P(AM1500−NIPAM10/10%) at 59 °C]. As a result, R_{HS} decreases from 390 Å at 3% to 310 Å at 5%.

Effect of Temperature. Experiments have been done with P(AM1500−NIPAM10/5%) at 33, 59, and 71 °C. At 35 °C, there is no aggregate and no peak. Above T^*, PNIPAM grafts form micelles and the mass fraction of grafts involved in the aggregation process increases with temperature, from 18% at 59 °C to 29% at 71 °C. As a result, the number density of micelles increases and, thus, R_{HS} decreases.

Copolymer Structure and Sieving Performances. In a previous article,[13] the optimal copolymer structure used as a medium for ssDNA separation was found to have a small graft size and graft density [P(AM1500-PNIPAM10/10%) at this time]. So, in regard to SANS experiments, performances get better when hydrophobic PNIPAM microdomains are minimized (smaller graft size or graft density). Indeed, the size of the domains increases with the graft size (R_{core} increases) and the number of domains per unit volume increases when the graft density increases (N_m increases with graft density). In both cases, there is more PNIPAM involved in aggregation (f_{PNIPAM} increases). Subsequently, the poor sieving properties of the copolymers with high f_{PNIPAM} may be due to hydrophobic interactions between microdomains of PNIPAM and ssDNA molecules, resulting in a dispersion of the sample zone during the separation process. Recently, Albarghouthi and Barron did show that an increased hydrophobicity of the sieving matrix is detrimental to the separation performance.[19] Here, the same trend seems to be observed, although extrapolation from a homogeneous matrix to a matrix with a hydrophilic network and hydrophobic domains was not obvious from the start. Increasing the copolymer's hydrophobicity by varying the temperature confirms this result. Indeed, the electrophoretic resolution is better in the transition range, in which the hydrophobicity of PNIPAM is still moderate (Figure 8). Above T^*,

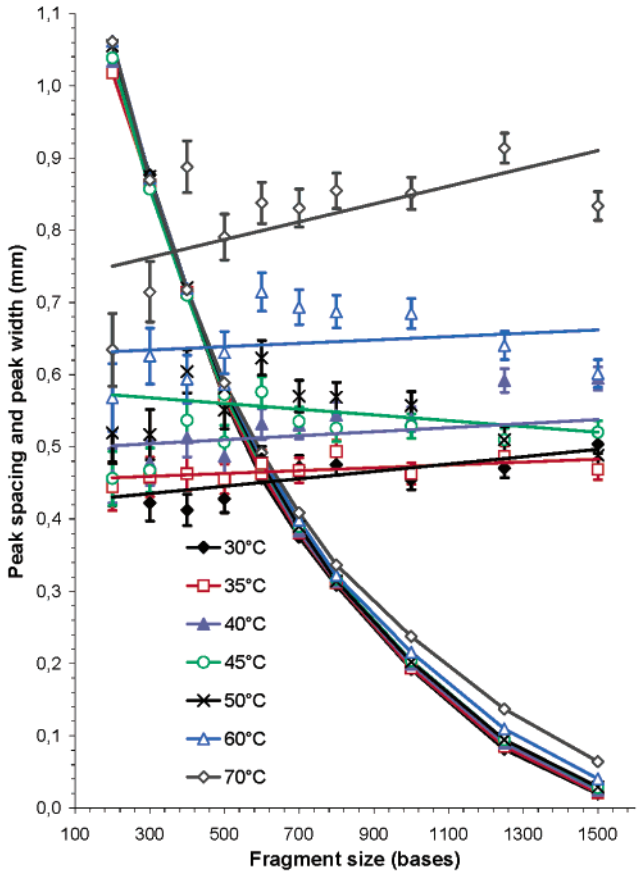

Figure 8. Separation of ssDNA (100−1500 b ladder) with P(AM1500−NIPAM10/10%), 3%, TTE, 7 M urea, 0.2% PDMA. Influence of the temperature on peak spacing and peak width: 200 V/cm, 50 cm length to detector, 75 μm capillary.

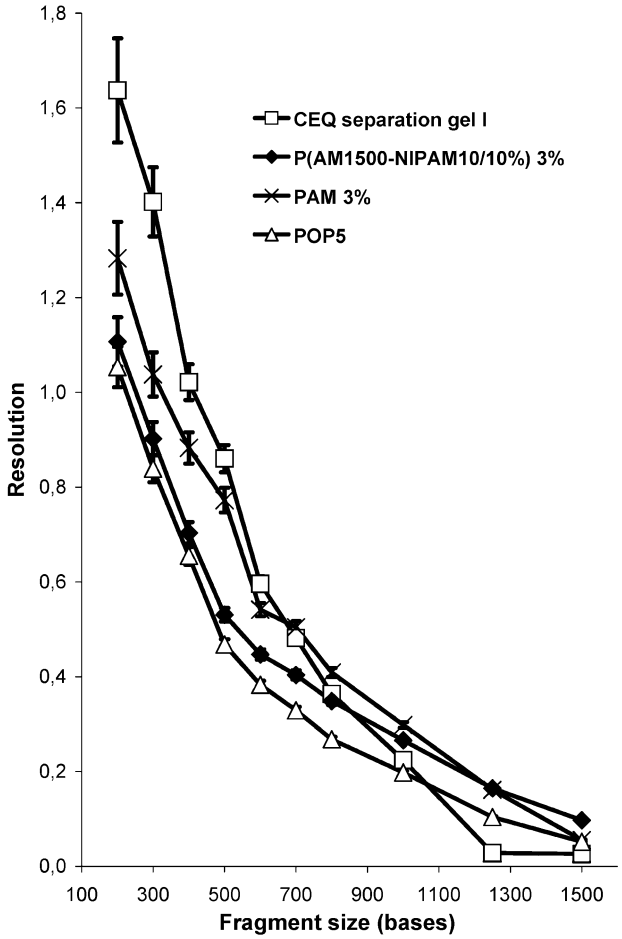

Figure 9. Separation of ssDNA (100−1500 b ladder) with P(AM1500−NIPAM10/10%), 3%. Comparison of resolution at equal-separation-time, state-of-the-art, commercial matrixes (PO5 and CEQ) and with a PAM 3% (10^6 g/mol). All separations performed at 50 °C.

sieving performances decrease with increasing temperature, that is, when micelle density and f_{PNIPAM} are more important. Despite this limitation, P(AM-*g*-PNIPAM) is an interesting matrix for DNA separation. In particular, it leads to sieving performances significantly better than those of POP5 (the matrix used in Applied Biosystems machines), which has a similar viscosity at room temperature, and for larger DNA fragments (>1250 bases) it is better than PAM with a similar molecular weight. As compared to CEQ separation gel I (Beckman Coulter), a matrix based on high-molecular-weight PAM with a very high viscosity, the resolution obtained with P(AM-*g*-PNIPAM) is lower for fragments smaller than 800 bases and better above 800 bases (Figure 9). We conclude that, for large DNA fragments, the positive effect of the thermo-thickening of the matrix is more important than the detrimental effect of DNA/matrix hydrophobic interactions. The opposite is true for small DNA fragments. This observation is consistent with the previous finding,[42] showing that large polyelectrolytes can deform weak matrixes more easily than smaller ones and reduce selectivity, so that the influence of the matrix strength on resolution increases with DNA size.

5. Discussion and Conclusion

In this paper, a SANS study on the aggregation behavior of PAM grafted with PNIPAM has been reported. In particular, we investigated the influence of graft size, graft density, polymer concentration, and temperature on the size (70−100 Å) and the number density of the aggregates (1.5×10^{-10} to 2.2×10^{-9} micelles/Å^3). We correlated the structural data with the copolymers' sieving properties for DNA sequencing. Several micellar models were used to fit the experimental results, and only the core−corona one yielded reasonable agreement with physically significant parameters for all data. The presence of a corona, inspired from the models developed for and applied with success to Pluronic triblock copolymers, may be questioned in our present system in which all the micelles are connected by a continuous PAM network. Nevertheless, we think that this corona reflects an increase of the PAM concentration in the vicinity of the micelles as a result of the attachment of PAM to the PNIPAM grafts (in average, the junction points play the role of an attractive force between PAM and the micelles). This conclusion is also consistent with the observation that the electrophoretic mobility of DNA in aggregated P(AM-*g*-PNIPAM) is higher than in long-chain PAM solutions at a given concentration, suggesting that the medium is more "open".

We also assumed that the core of the micelles is totally dry and contains only a fraction of PNIPAM chains. The opposite assumption ("wet" micelles containing all the PNIPAM) was not consistent with the data, but this does not rule out the possibility of a combination of a wet core and nonmicellized free PNIPAM, in particular in the transition zone in which PNIPAM is only moderately hydrophobic. Some ele-

ments of the data actually suggest that it may be the case. In particular, the DSC results (Figure 4) lead to a dehydration enthalpy of 0.4 kJ/mol, which would correspond to 6−7% of totally dehydrated micelles (when compared to the pure PNIPAM case), whereas the SANS data in the same conditions lead to a higher number, of about 23% of PNIPAM involved in micelles. This discrepancy would suggest that the PNIPAM in the micelles is actually not fully dehydrated. Unfortunately, we were not able to include this possibility into our fitting, because combining wet micelles and incomplete incorporation of PNIPAM into the micelles would have led to a six-free-parameters fit. Considering the accuracy of the data, and the strong coupling between some parameters in the fit, this was beyond what one could reasonably and consistently extract from the data. Despite this limitation, the rather good fit obtained with the model assuming dry micelles and free PNIPAM (much better than obtained, e.g., with wet micelles and no free PNIPAM) suggests that the structural parameters obtained within this model are reasonably close to reality. In this model, the mass fraction f_{PNIPAM} of grafts involved in aggregates varies from 18 to 50% depending on the copolymer. As expected, f_{PNIPAM} is highest at high temperatures and for a copolymer with a higher graft size or density.

Concerning the use of P(AM-*g*-PNIPAM) as a matrix for DNA separation, this SANS study is consistent with the detrimental effect of the hydrophobic microdomains on the separation performances for medium-sized DNA. We expect that increased hydrophobic interactions between aggregates and DNA leads to a peakdispersion and, consequently, to loss in separation. However, for larger fragments, this negative effect is overcompensated by the increase in resolution due to matrix gelation, and rather promising performances were obtained in comparison with commercial matrixes.

Acknowledgment. V.B. acknowledges a Ph.D. grant from Association pour la Recherche sur le Cancer (ARC). We are grateful to Genoscope, Evry, France, for the generous loan of an ABI 310. This work was partly supported by EU Project No. QLG2-2001-01903, ARC (Association pour la Recherche sur le Cancer) Grant 4374, and funding by FNS (French National Fund for Science) to project “Actipols”.

References and Notes

(1) Sarkar, N. J. *J. Appl. Polym. Sci.* **1979**, *24*, 1073.
(2) Carlsson, A.; Karlstrom, G. *Colloids Surf.* **1990**, *47*, 147.
(3) Aubry, T. *J. Rheol.* **2003**, *47*, 577.
(4) Virtanen, J. *Macromolecules* **2000**, *33*, 5970.
(5) Maroy, P.; Hourdet, D.; L'Alloret, F.; Audebert, R. European Patent 0 583 814 A1, 1993.
(6) Hourdet, D.; L'Alloret, F.; Audebert, R. *Polymer* **1997**, *38*, 2535.
(7) Durand, A. Thesis, Université Pierre et Marie Curie, Paris, France, 1998.
(8) Bromberg, L. *Macromolecules* **1998**, *31*, 6148.
(9) Durand, A. *Polymer* **1999**, *40*, 4941.
(10) Virtanen, J.; Baron, C.; Tenhu, H. *Macromolecules* **2000**, *33* (2), 336.
(11) Virtanen, J.; Tenhu, H. *Macromolecules* **2000**, *33* (16), 5970.
(12) Qiu, X.; Wu, C. *Macromolecules* **1997**, *30* (25), 7921.
(13) Sudor, J.; Barbier, V.; Thirot, S.; Godfrin, D.; Hourdet, D.; Millequant, M.; Blanchard, J.; Viovy, J. L. *Electrophoresis* **2001**, *22*, 720.
(14) Bashkin, J.; Marsh, M.; Barker, D.; Johnston, R. *Appl. Theor. Electrophor.* **1996**, *6*, 23.
(15) Liu, W. G. Y.; Kuhr, W. G. *Anal. Chem.* **1999**, *71*, 1668.
(16) Madabhushi, R. S. *Electrophoresis* **1998**, *19*, 224.
(17) Kim, Y.; Yeung, E. S. *Electrophoresis* **1997**, *18*, 2901.
(18) Gao, E. S. Q.; Yeung, E. S. *Anal. Chem.* **1998**, *70*, 1382.
(19) Albarghouthi, M. N.; Barron, A. E. *Electrophoresis* **2000**, *21*, 4096.
(20) Carrilho, E. *Electrophoresis* **2000**, *21*, 55.
(21) Barbier, V.; Viovy, J. L. *Curr. Opin. Biotechnol.* **2003**, *14*, 51.
(22) Buchholz, B. A.; Shi, W.; Barron, A. E. *Electrophoresis* **2002**, *23*, 1398.
(23) Carrilho, E.; Ruiz-Martinez, M. C.; Berka, J.; Smirnov, I.; Goetzinger, W.; Miller, A. W.; Brady, D.; Karger, B. L. *Anal. Chem.* **1996**, *68*, 3305.
(24) Goetzinger, W.; Kotler, L.; Carrilho, E.; Ruiz-Martinez, M. C.; Salas-Solano, O.; Karger, B. L. *Electrophoresis* **1998**, *19*, 242.
(25) Salas-Solano, O.; Carrilho, E.; Kotler, L.; Miller, A. W.; Goetzinger, W.; Sosic, Z.; Karger, B. L. *Anal. Chem.* **1998**, *70*, 3996.
(26) Zhou, H.; Miller, A. W.; Sosic, Z.; Buchholz, B.; Barron, A. E.; Kotler, L.; Karger, B. L. *Anal. Chem.* **2000**, *72*, 1045.
(27) Liang, D.; Song, L.; Zhou, S.; Zaitsev, V. S.; Chu, B. *Electrophoresis* **1999**, *20*, 2856.
(28) Liu, T.; Liang, D.; Song, L.; Nace, V. M.; Chu, B. *Electrophoresis* **2001**, *22*, 449.
(29) Liang, D.; Chu, B. *Electrophoresis* **1998**, *19*, 2447.
(30) Wu, C.; Liu, T.; Chu, B. *Electrophoresis* **1998**, *19*, 231.
(31) Wu, C.; Liu, T.; Chu, B.; Schneider, D. K.; Graziano, V. *Macromolecules* **1997**, *30*, 4574.
(32) Goldmints, I.; Von Gottberg, F. K.; Smith, K. A.; Hatton, T. A. *Langmuir* **1997**, *13*, 3659.
(33) Jain, N. J.; Aswal, V. K.; Goyal, P. S.; Bahadur, P. *J. Phys. Chem. B* **1998**, *102*, 8452.
(34) Goldmints, I.; Yu, G. E.; Booth, C.; Smith, K. A.; Hatton, T. A. *Langmuir* **1999**, *15*, 1651.
(35) Yang, L.; Paschalis, A.; Steytler, D. C.; Kositza, M. J.; Holzwarth, J. F. *Langmuir* **2000**, *16*, 8555.
(36) Isambert, H. Thesis, Université de Paris 11, Orsay, France, 1996.
(37) Hourdet, D.; L'Alloret, F.; Durand, A.; Lafuma, F.; Audebert, R.; Cotton, J. P. *Macromolecules* **1998**, *31*, 5323.
(38) Carrilho, E.; Ruiz-Martinez, M. C.; Berka, J.; Smirnov, I.; Goetzinger, W.; Miller, A. W.; Brady, D.; Karger, B. L. *Anal. Chem.* **1996**, *68*, 3305.
(39) Cotton, J. P. In *Neutrons, X-ray and light scattering*; Lindner, P., Zem, T., Eds.; Elsevier: North-Holland, 1991; pp 1−31.
(40) Kreig, A.; Lefebvre, A. A.; Hahn, H.; Balsara, N. P.; Qi, S.; Chakraborty, A. K.; Xenidou, M.; Hadjichristidis, N. *J. Chem. Phys.* **2001**, *115*, 6243.
(41) Hansen, J. P.; McDonald, I. R. *Theorie of Simple Liquids*, 2nd ed.; Academic Press: New York, 1986.
(42) Cottet, H.; Gareil, P.; Viovy, J. L. *Electrophoresis* **1998**, *19*, 2151.

MA049182Y